Divacancy in 3*C*- and 4*H*-SiC: An extremely stable defect

L. Torpo,* T. E. M. Staab,† and R. M. Nieminen‡
Laboratory of Physics, Helsinki University of Technology, P.O. Box 1100 FIN-02015 HUT, Finland
(Received 27 August 2001; published 30 January 2002)

Using first-principles calculations for divacancy defects in 3*C*- and 4*H*-SiC, we determine their formation energies and stability, their ionization levels, and relaxed geometries (symmetry point groups) for neutral as well as for charged states. For 4*H*-SiC all four possible nearest-neighbor divacancy configurations are considered. We find not only a remarkable high binding energy of about 4 eV, but also a strong site dependence (cubic or hexagonal lattice sites) of the formation energies. Applying a Madelung-type correction to deal with the electrostatic interactions between charged supercells, our results indicate a negative-*U* behavior at $E_V + 0.7$ eV between the charge states $1+/1-$ only for nearest-neighbor divacancies on different lattice sites (mixed cubic and hexagonal) in 4*H*-SiC, but not for all the other cases (pure cubic or pure hexagonal) in 4*H*- or for the cubic divacancy in 3*C*-SiC.

DOI: 10.1103/PhysRevB.65.085202 PACS number(s): 71.20.Nr, 61.72.Ji

I. INTRODUCTION

SiC is a very promising material for semiconductor device applications which have to work under extreme conditions. Due to its good thermal conductivity, its high radiation resistance, and high breakdown voltage, it is well suited for demanding applications in harsh environments.

Even though progress in crystal growth during the past years has been able to reduce imperfection in SiC to a great extent, many properties of grown-in defects or those produced by irradiation damage are not well understood. However, new defects are introduced during doping wafers by ion implantation. To get rid of unwanted damage and to bring the dopant atoms on lattice sites—to activate them—one has to employ certain annealing steps, where unnecessarily high temperatures have to be avoided, since this would cause the dopants to diffuse and the sharp ion implantation profile would be lost. During annealing, irradiation-induced defects may or may not anneal out. In the ''hard'' SiC most primary defects are stable at room temperature and, hence, are easily accessible experimentally.

Since defects of the crystal lattice influence the electrical properties of the material, there is a great need to identify and to understand them. In the past there were difficulties in understanding the electric properties of GaAs, due to the electrically active point defect EL2, existing even in as-grown crystal in high concentrations. Now—after more than 20 years of studies—consensus has been reached on EL2 being the the isolated As antisite in GaAs. To improve the reliability of defect identification, it is necessary to compare experimental data on defect symmetries, formation energies, and ionization levels to first-principles calculations. Defect identification is the prerequisite to avoid or—if unwanted—to deactivate them.

A characteristic property of SiC is its polymorphism—an uncommon feature in nature. Polymorphism means that SiC is able to crystallize in different modifications, so-called polytypes. The polytypes differ in the stacking sequence of hexagonally close-packed double layers of Si and C atoms. Depending on the next-nearest-neighbor atom arrangement, the atom sites in SiC crystal are classified to be cubic or hexagonal ones. In 4*H*-SiC the divacancy $V_{Si}V_C$—formed by nearest-neighbor silicon (V_{Si}) and carbon (V_C) monovacancies—has four possible configurations, since both Si and C atoms can be located either in cubic (''cub'') or hexagonal (''hex'') lattice sites. The four possible configurations are $V_{Si}^{cub}V_C^{cub}$, $V_{Si}^{cub}V_C^{hex}$, $V_{Si}^{hex}V_C^{cub}$, and $V_{Si}^{hex}V_C^{hex}$. In 3*C*-SiC, on the other hand, there is only one kind of lattice site, the cubic one, and thus only one kind of divacancy $V_{Si}^{cub}V_C^{cub}$.

Already identified intrinsic point defects in SiC such as the silicon and carbon vacancies (V_{Si}, V_C) or the silicon antisite Si_C cannot explain the high thermal stability of a number of commonly detected photoluminescence (PL) centers in SiC.[1,2] Since the presence of simple point defects (vacancies, interstitials, antisites) can be excluded, one has to look for more extended defects—the simplest examples are the divacancy or vacancy-antisite pairs.

Although the divacancy $V_{Si}V_C$ has experimentally not been conclusively identified in SiC, it has in the past often been proposed to be an important defect center. Hence, there is a must to study the divacancy in 3*C*- and 4*H*-SiC by first-principles calculations. The Z_1 and Z_2 defect centers observed by various capacitance transient techniques[3–6] and photoinduced electron spin resonance[7] (ESR) have been proposed to be associated with $V_{Si}V_C$.[3,7] Also for one of the most common and stable defect centers in SiC labeled $D1$–widely detected in PL studies[8–13]— the divacancy has been discussed in the past as a possible candidate.[8–10,14] However, no full consensus prevails regarding the origin of $D1$.[12] In the experimental literature, divacancy-related defect centers are discussed also in several positron annihilation studies (cf., e.g., Refs. 15–17).

In computational studies for defect properties in SiC, the electronic structure of the divacancy in SiC has received little attention up to now. While Talwar and Feng[14] used a semiempirical tight-binding (TB) approach for a divacancy in 3*C*-SiC, Wang *et al.*[18] studied the electronic structure of the divacancy with *ab initio* methods, where the calculations were performed in 3*C*-SiC using a 32-atom supercell without full ionic relaxations. The TB study by Talwar and

 ©2002 The American Physical Society

Feng[14] revealed that the divacancy has localized impurity states in the semiconductor gap. The symmetry point group was determined to be C_{3v} for the neutral divacancy,[14] whereas in the *ab initio* study the formation energy was evaluated to be 8.1 eV.[18]

Even though for many point defects in SiC (antisites, monovacancies, and antistructure pairs) accurate pseudopotential calculations, employing full ionic relaxations[19–22] and large (128 or 216 atom) supercells, have appeared during past years, the electronic structure of the divacancy in SiC has not been studied recently using accurate state-of-the-art first-principles methods. In this paper, the electronic structure of all nearest-neighbor divacancies in $3C$- and $4H$-SiC polytypes will be studied. While the electronic structure of the divacancy in GaAs and Si has been successfully studied using plane-wave pseudopotential calculations,[23,24] to the knowledge of the authors, no works have been reported on divacancies in SiC.

II. METHODS

Our calculations are based on the density-functional theory (DFT) with the electron exchange correlation treated in the local density approximation[25] (LDA) and local spin density approximation (LSDA).[26] We have used a Car-Parrinello-like pseudopotential approach.[27] While for the C ion the Vanderbilt-type ultrasoft pseudopotential[28] has been employed in order to reduce the number of plane waves needed to describe the electronic wave functions, a standard norm-conserving Bachelet-Hamann-Schlüter pseudopotential[29] has been used for the Si ion. Good convergence with respect to the basis set size is obtained at a 20 Ry kinetic energy cutoff,[30] which has been used throughout this work. In the defect calculations, the initial atomic configurations have been randomized slightly from the ideal structure to remove any spurious symmetries. All the ions in the supercell have been allowed to relax without any symmetry constraints using the Broyden-Fletcher-Goldfarb-Shanno (BFGS) algorithm.[31] For the electronic structure minimization, we employ damped second-order dynamics[32] combined with the Williams-Soler algorithm.[33] All calculations have been performed in a massively parallel CRAY-T3E system using the carefully optimized FINGER (finnish general electron relaxator) code.[34] While in $3C$-SiC the calculations are performed for a 128-atom-site fcc supercell, for the hexagonal structure of $4H$-SiC the supercell is elongated in the c direction due to the ratio $c/a=1.63$. Hence, to keep the distance between the defect and its periodic replica in the superlattice as large as possible, we choose—after carefully testing other alternatives—a rectangular supercell having a shape close to cubic (the hexagonal lattice of $2H$-, $4H$-, and $6H$-SiC can be transferred to cubic coordinates resulting in rectangular supercell). In all calculations a rectangular 128-atom supercell has been employed. Considering a proper **k**-point set,[35] use of the Γ point provides sufficiently well-converged results as well as the required efficiency in computing.[19,30] For spin-unpaired charge states (V_2^{1+} and V_2^{1-}), we performed a spin-polarized calculation employing the LSDA scheme.[26]

A. Formation energies for defects

The formation energy of defects $E_F(q)$ is calculated using the standard formalism by Zhang and Northrup.[36] For all positions of the electron chemical potential and the possibly appearing stoichiometries between C- and Si-rich compounds, the formation energy $E_F(q)$ is defined as follows:

$$\begin{aligned} E_F(q) &= E_{tot}(q) + q(E_V+\mu_e) - n_{Si}\mu_{Si} - n_C\mu_C \\ &= E_{tot}(q) - \frac{1}{2}(n_{Si}+n_C)\mu_{SiC}^{bulk} - \frac{1}{2}(n_{Si}-n_C)(\mu_{Si}^{bulk} \\ &\quad - \mu_C^{bulk}) + q(E_V+\mu_e) - \frac{1}{2}(n_{Si}-n_C)\Delta\mu, \end{aligned} \tag{1}$$

where $E_{tot}(q)$ is the total energy of the defect supercell in question and q the charge state. n_{Si} and n_C are the numbers of Si and C atoms in the supercell, respectively. μ_e is the electron chemical potential measured relative to the valence-band maximum E_V. μ_{Si}^{bulk} and μ_C^{bulk} are the chemical potentials of the Si and C atoms in the bulk Si and C lattices, respectively. μ_{SiC}^{bulk} is the chemical potential of the SiC pair in the bulk SiC compound. Actually it is possible to know only

$$\mu_{SiC}^{bulk} = \mu_{Si} + \mu_C, \tag{2}$$

not the chemical potentials μ_{Si} and μ_C of the single atom separately. This fact is circumvented in Eq. (1) by introducing the chemical potential difference

$$\Delta\mu = (\mu_{Si} - \mu_C) - (\mu_{Si}^{bulk} - \mu_C^{bulk}). \tag{3}$$

The allowed range of $-\Delta H < \Delta\mu < \Delta H$ is determined from the calculated heat of formation for SiC defined as

$$\Delta H = \mu_{Si}^{bulk} + \mu_C^{bulk} - \mu_{SiC}^{bulk}. \tag{4}$$

The atomic chemical potential difference $\Delta\mu$ determines the deviation from the ideal stoichiometry. It can vary from $-\Delta H$ (C rich) to ΔH (Si rich).

We plot the formation energies as functions of the electron chemical potential from the valence-band maximum (VBM) E_V to the value of the band gap (E_{gap}). The appropriate value for the chemical potential difference $\Delta\mu$ depends on the defect and the defect formation process.

The ionization level (q/q') of a given defect is the position of μ_e in the band gap where the most stable charge state changes from q to q'. Ionization levels can be obtained by solving the following equation for the value of the electron chemical potential μ_e:

$$E_{tot}(q) + q(E_V+\mu_e) = E_{tot}(q') + q'(E_V+\mu_e). \tag{5}$$

The computational DFT-LSDA method has some unresolved problems, which can have a significant influence on the ionization levels. The most important is the gap problem: in the electronic structure calculations the band gap is extracted from Kohn-Sham single-particle energy levels. For-

mally, these levels do not describe any physical quantity—only the total energy is well defined. Although Kohn-Sham eigenvalues sometimes agree quite nicely with the true quasiparticle band structure, the width of the band gap is always severely underestimated. While the corresponding experimental values for 3*C*- and 4*H*-SiC are $E_g = 2.39$ and 3.27 eV, respectively, we obtain for the energy gap of 3*C*- and 4*H*-SiC $E_g = 1.24$ and 2.6 eV, respectively. Since defect states appear in the band gap, there can be problems in interpreting the actual positions of the ionization levels according to Eq. (5). In this work, the calculation of the ionization levels is based on the total energies. We will consistently report ionization levels measured from the valence-band maximum. However, when plotting the formation energies, we indicate also the position of the LDA gap and leave it to the reader to measure the distance of an ionization level with respect to the experimental conduction-band minimum (CBM) or with respect to the Kohn-Sham band edge.

Neglecting the phonon contribution to the entropy, the defect concentration C is given as a function of the formation energy, for a given electron chemical potential μ_e and a stoichiometry $\Delta\mu$, at temperature T by the formula

$$C = zN_s \exp[-E_F(q,\mu_e,\Delta\mu)/(k_B T)], \tag{6}$$

where z is the number of different possible configurations for a defect per the sublattice site, N_s is the number of the sublattice sites per unit volume, E_F is the formation energy, q is the charge state, and μ_e the electron chemical potential, while $\Delta\mu$ describes the deviation from the ideal stoichiometry (Si rich or C rich).

B. Madelung correction

In charged supercell calculations a compensating background has to be introduced. The spurious electrostatic interactions between repeated cells give rise to a correction in the total energy depending inversely on the cell dimension L and on the square of its charge q^2. This introduces minor problems for singly positive- and negative-charge states, whereas for doubly negative- or positive-charge states the error is significantly larger. It is nontrivial to calculate the correction. Hence, we use here the heuristic approach introduced by Makov and Payne for the error evaluation,[37] which has been successfully applied in a recent study leading to a good agreement between calculated and experimentally determined ionization levels of point defects in SiC.[30]

Using this formalism, the electrostatic corrections for the formation energy are evaluated in the following way

$$E = E_0 - \frac{q^2\alpha}{2L\epsilon} - \frac{2\pi qQ}{3L^3\epsilon} + 0(L^5), \tag{7}$$

where the E_0 is the total energy of the supercell obtained from the calculations, Q is the quadrupole moment of the charge distribution in the supercell, $\alpha = 1.418\,65$ (rectangular 128-atom cell of size 19.89 a.u.) the Madelung constant, $\epsilon = 6.7$ the experimental dielectric constant, and L the size of used supercell. The contribution arising from the second term of the Madelung correction is only one-third of that coming from the first correction term.[38] Since this may be beyond the accuracy of the method, it will not be considered here. For 4*H*-SiC, we obtain a correction for $q = \pm 1$ around 0.3 eV and for $q = \pm 2$ about 1.2 eV.

TABLE I. Monovacancies and divacancies in 4*H*- and 3*C*-SiC: shown are the calculated formation energies E_F in electron volts [eV]. In 4*H*-SiC, E_F is evaluated for all possible, cubic (cub) or hexagonal (hex), lattice sites. The values of the formation energy are given for stoichiometric ($\Delta\mu = 0$) SiC. A remarkable high binding energy E_b is obtained for all divacancies.

	Monovacancies				Divacancies		
	V_{Si}		V_C		$V_{Si}V_C$		
	E_F [eV]		E_F [eV]		Type	E_F [eV]	E_b [eV]
	4*H*-SiC						
Site	cub	hex	cub	hex			
	8.37	—	4.07	—	$V_{Si}^{cub}V_C^{cub}$	7.74	4.36
	8.37	—	—	4.21	$V_{Si}^{cub}V_C^{hex}$	8.34	3.90
	—	8.26	4.07	—	$V_{Si}^{hex}V_C^{cub}$	8.36	3.77
	—	8.26	—	4.21	$V_{Si}^{hex}V_C^{hex}$	8.00	4.27
	3*C*-SiC						
	7.79	—	2.77	—	$V_{Si}V_C$	7.22	3.34

III. RESULTS

A. Formation energies

In Table I, we present our results for the formation energies of mono- and divacancies in 3*C*- and 4*H*-SiC under stoichiometric conditions ($\Delta\mu = 0$). The binding energies for the neutral divacancy defects in 3*C*- and 4*H*-SiC are given for all lattice site configurations in Table I as well.

We find the lowest formation energies for divacancies in 4*H*-SiC when both V_{Si} and V_C are along the c axis (both vacancies either only on cubic or only on hexagonal lattice sites). The by-far lowest formation energy is obtained for the pure cubic lattice site: $V_{Si}^{cub}V_C^{cub}$. The values are 7.22 eV for 3*C*-SiC and 7.74 eV for 4*H*-SiC, while for a purely hexagonal divacancy in 4*H*-SiC, $V_{Si}^{hex}V_C^{hex}$, we find a somewhat higher formation energy of 8.0 eV. By far the highest formation energies are those for the mixed cases $V_{Si}^{cub}V_C^{hex}$ and $V_{Si}^{hex}V_C^{cub}$ (divacancies not along the c axis in 4*H*-SiC), where the formation energy E_F is 0.6 eV larger than the pure cubic case (see Table I).

It has to be pointed out that the formation energy of divacancies on pure cubic or pure hexagonal lattice sites is in fact lower than the formation energy of isolated silicon monovacancies on corresponding lattice sites (see Table I for stoichiometric material). For the pure cubic divacancy this energy difference is as high as 0.6 eV, while for the pure hexagonal divacancy it is about 0.3 eV. Due to this signifi-

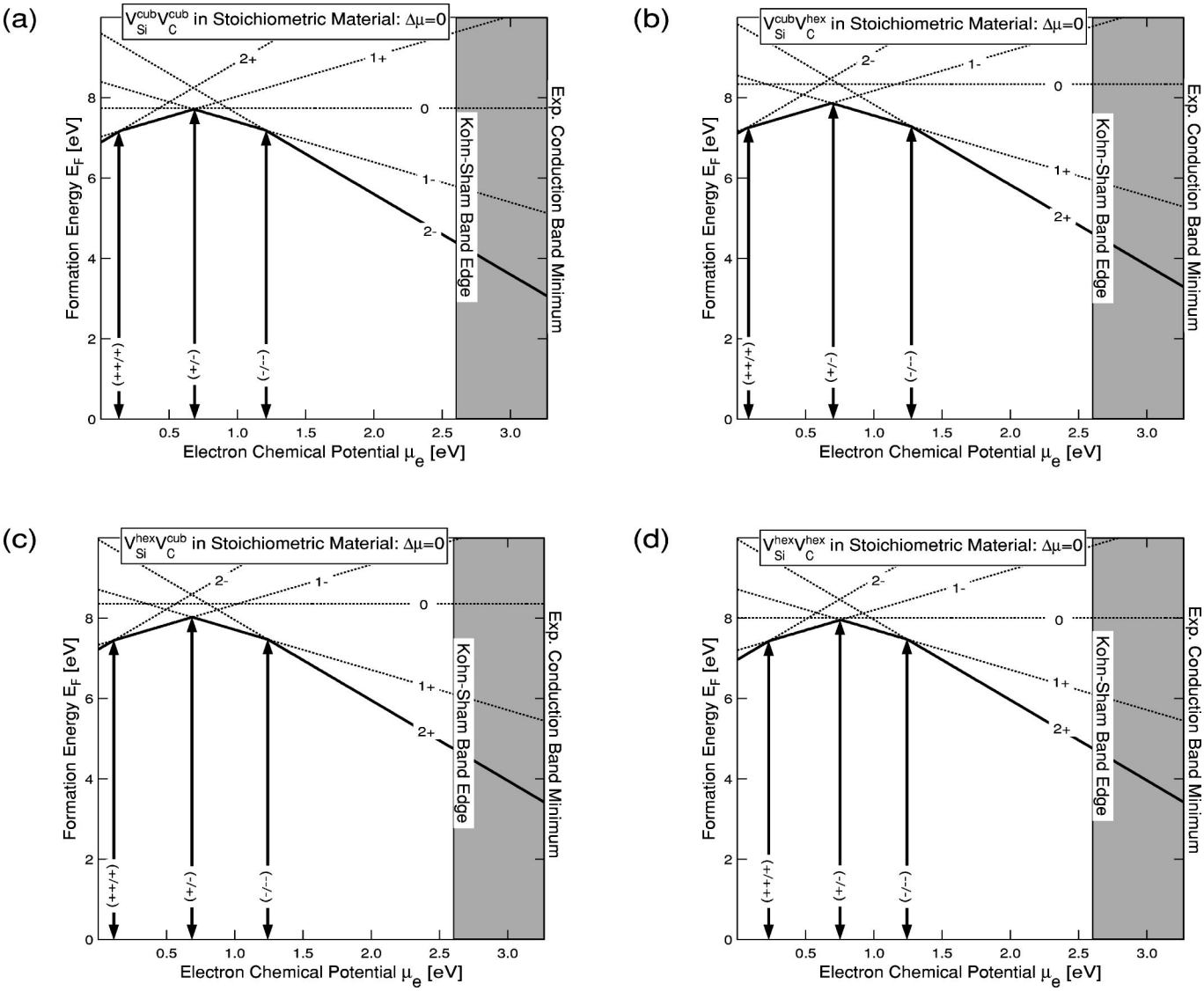

FIG. 1. $V_{Si}V_C$: divacancies in 4H-SiC in all possible site configurations for stoichiometric material ($\Delta\mu=0$). Formation energies E_F vs the electron chemical potential $\Delta\mu_e$ are given for different charge states (dashed lines), with each charge state indicated. The thick solid line corresponds to the lowest formation energy for all values of the electron chemical potential. The ionization levels (indicated by arrows in the picture) are at the intersection of dashed lines. Note the negative-U effect found between charge state $(-/+)$ at the value of 0.68 eV of electron chemical potential.

cant difference, one may expect to find a higher concentration of divacancies than the corresponding one of isolated silicon monovacancies under equilibrium conditions according to Eq. (6).

Since the formation energy for divacancies is low compared to monovacancies, we also find an extraordinarily large binding energy (3.8–4.4 eV) between vacancies on different sublattices in 4H-SiC (see Table I). The pure cubic or the pure hexagonal cases have the highest binding energy. They are larger by about 0.6 eV compared to the mixed ones. The cases where the silicon vacancy on a cubic lattice site is involved—either pure or mixed—are favored by about 0.1 eV. Additionally, the pure cubic case is favored compared to the pure hexagonal one by a difference in the formation energy of 0.26 eV. Again we see a strong site dependence.

For 3C-SiC the binding energy found is significantly smaller: about 3.3 eV. This is in qualitative agreement with previous calculations by Wang *et al.*, employing only a 32-atom supercell, where the binding energy was evaluated to be 4.6 eV in 3C-SiC.[18]

B. Ionization levels

In Fig. 1 the formation energies for all possible nearest-neighbor (NN) divacancies in 4H-SiC are given as a function of the electron chemical potential without any correction. The ionization level $(1+/2+)$ is located just above the VBM for 4H-SiC while it is slighly higher for 3C-SiC. The ionization level $(2-/1-)$ is situated slightly below midgap. A negative-U behavior between the $(1-/1+)$ charge states is found generically for 4H-SiC at about 0.7 eV above the

TABLE II. Divacancies in 4*H*- and 3*C*-SiC: ionization levels for the relaxed defects. The results from LSDA calculations are given in eV above the valence-band maximum. The upper part is without any correction, while in the lower part the Madelung correction is applied. In 4*H*, the results are given for all four nearest-neighbor divacancy combinations. The unphysical states are given in brackets. Depending on the type of the divacancy, there is a minor deviation in the position of the negative-*U* transition.

	Ionization levels [eV] above the VBM				
			Neg.-*U*		
Defect	2+/1+	1+/0	1+/1−	0/1−	1−/2−
Without correction					
4*H*: $V_{Si}^{cub}V_C^{cub}$	0.14	(0.71)	**0.68**	(0.65)	1.20
4*H*: $V_{Si}^{cub}V_C^{hex}$	0.11	(1.02)	**0.69**	(0.36)	1.24
4*H*: $V_{Si}^{hex}V_C^{cub}$	0.06	(1.17)	**0.69**	(0.22)	1.28
4*H*: $V_{Si}^{hex}V_C^{hex}$	0.23	(0.80)	**0.76**	(0.71)	1.25
3*C*: $V_{Si}V_C$	0.42	(1.00)	**0.85**	(0.70)	1.16
Madelung correction applied					
4*H*: $V_{Si}^{cub}V_C^{cub}$	—	0.52	—	0.85	1.76
4*H*: $V_{Si}^{cub}V_C^{hex}$	—	(0.98)	**0.69**	(0.41)	1.84
4*H*: $V_{Si}^{hex}V_C^{cub}$	—	(0.83)	**0.69**	(0.55)	1.80
4*H*: $V_{Si}^{hex}V_C^{hex}$	—	0.61	—	0.90	1.81
3*C*: $V_{Si}V_C$	—	0.81	—	0.89	1.72

VBM for all cases [see Figs. 1(a)–1(d)], while for 3*C*-SiC it is about 0.85 eV above the VBM [see Fig. 3(a)]. For details see Table II.

If the Madelung correction is applied, the picture changes in some important aspects. As we can see from Figs. 2(a)–2(d), the 2+ charge state is not stable anymore; i.e., it vanishes to the valence band. In turn the stability region of the single positive-charge state of the divacancy 1+ becomes wider and extends from the VBM to about $E_V+0.5$–0.7 eV. Due to the correction, the ionization level (2−/1−) has moved higher up in the band gap and is now found at about $E_V+1.8$–2.0 eV above the VBM for both 4*H*- and 3*C*-SiC. For 3*C*-SiC this means that the (2−/1−) level is now found above the Kohn-Sham band edge but still below the experimental CBM. Hence, the charge state 1− extends over a wide region around midgap—from $E_V+0.7$ eV up to $E_V+1.8$ eV for 4*H*-SiC and from $E_V+0.9$ eV up to $E_V+1.7$ eV for 3*C*-SiC. For 4*H*-SiC our results indicate that the charge state 2− is stable even with the applied Madelung correction, provided that the value of the electron chemical potential is high (*n*-type material). For details see Table II.

Concerning the negative-*U* behavior in 4*H*-SiC, it is still found for the mixed case (one of the vacancies is on a cubic site and the other on a hexagonal site—$V_{Si}^{hex}V_C^{cub}$ or $V_{Si}^{hex}V_C^{cub}$). For the pure cubic or pure hexagonal case (divacancies formed along the *c* axis: $V_{Si}^{cub}V_C^{cub}$, $V_{Si}^{hex}V_C^{hex}$), on the other hand, by applying the Madelung correction the neutral state stabilizes over a wide range of the electron chemical potential and the negative-*U* behavior is removed. The reason for this different behavior can be found in the lower formation energy of the charge-neutral divacancy in the latter cases and, hence, the neutral-charge state stabilizes in the range $E_V+(0.5$–$0.9)$ eV. This means that all charge states from 1+ to 2− may stabilize for certain values of the electron chemical potential.

For the nearest-neighbor divacancy in 3*C*-SiC the negative-*U* behavior between the 1+ and 1− charge state [see Fig. 3(a)] is removed when the Madelung correction is applied and the neutral divacancy may stabilize in a small range of the electron chemical potential [see Fig. 3(b)].

C. Relaxations

The relaxations of the atoms surrounding the different divacancies are listed in Table IV below. The relaxations of the three Si atoms sitting around one end (carbon vacancy) are denoted by the bond lengths between them, d_{12},d_{13},d_{23}. Respectively, the bonds between the C atoms surrounding the other end of the divacancy (around the missing Si atom) are denoted by d_{45},d_{46},d_{56}. For 4*H*-SiC the symmetry groups are given considering only the NN arrangements, i.e., provided that there is locally a mirror plane or a rotational symmetry.

Generally we find a strong outward relaxation of the C atoms around the missing Si atom (V_{Si} in $V_{Si}V_C$), while the Si atoms around the missing C atom (V_C in $V_{Si}V_C$) are only slightly moved—after the relaxation they are found nearly in their ideal places. In detail, we can describe the relaxation around the divacancy in the charge states 2+ or 2− by a *breathing-mode* type or weak pairing type according to the obtained symmetry group C_{3v}. For singly negative- or positive-charge states the relaxation is found to be mostly of the *pairing type* (symmetry group C_{1h}). The neutral-charge state—according to our results—is not stable in all cases. It tends to have the *resonant-bond*-type relaxation (symmetry group C_{1h}).

Comparing to the relaxation patterns obtained for monovacancies[20,22,30] in 3*C*- and 4*H*-SiC we note the following: The C atoms around the silicon monovacancy V_{Si} relax outward ~10% in T_d or C_{3v} symmetry for all polytypes. The relaxations around the missing silicon atom in $V_{Si}V_C$ are more distorted, and the outward movement is not as large as in the case of the silicon monovacancy. For the carbon monovacancy V_C a Jahn-Teller-distorted, pronounced inward relaxation is found,[22,30] whereas—as already noted—for V_C in $V_{Si}V_C$ the Si atoms stay nearly at their ideal lattice positions.

IV. DISCUSSION

A. Formation energies

Due to the wide band gap of SiC (experimental values are $E_g=2.4$ eV for 3*C*-SiC and 3.3 eV for 4*H*-SiC), the for-

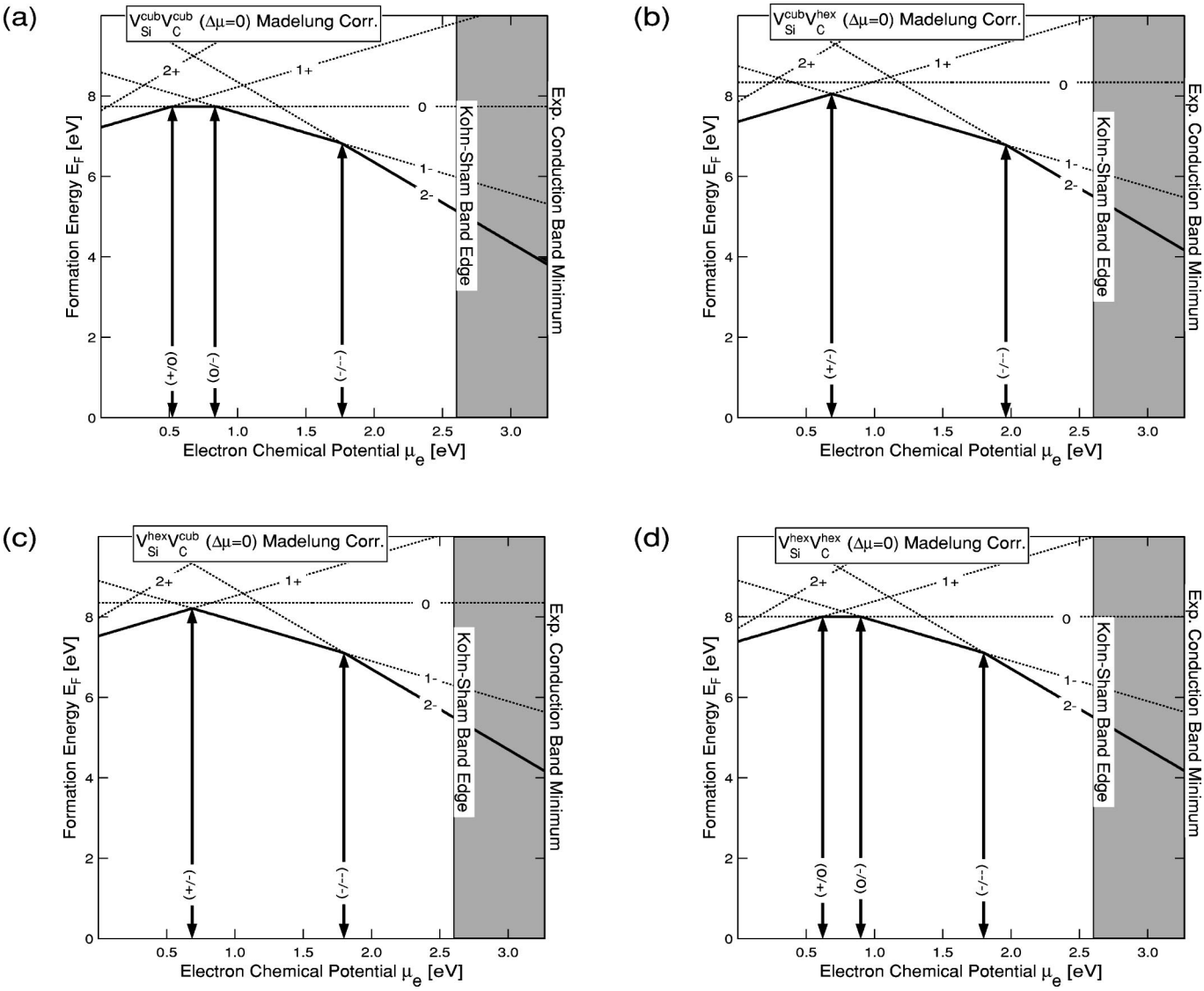

FIG. 2. $V_{Si}V_C$: divacancy in 4H-SiC in all possible site configurations for stoichiometric material ($\Delta\mu=0$). Just like the figure above only the Madelung correction is applied. Note that the negative-U effect is removed for the pure cubic or pure hexagonal case.

mation energies of defects depend heavily on the position of the electron chemical potential [see Eq. (1)]. In hexagonal polytypes, such as 4H-SiC, the band gap is about 1 eV wider than in cubic 3C-SiC, which favors negative-charge states (theoretical values are $E_g=1.24$ eV for 3C-SiC and 2.6 eV for 4H-SiC).

Considering the site dependence on the formation energies for monovacancies, it turns out that the energy differences are smaller than 0.1 eV (see Table I and Ref. 30). But for divacancies the story is different: there we find a strong dependence on the lattice sites (cubic or hexagonal) from which the atoms have been removed. The most expensive divacancies are for mixed cases (one vacancy from a cubic site and the other from a hexagonal site). If, on the other hand, both silicon and carbon atoms are removed from hexagonal sites, the formation energy is smaller by about 0.35 eV, while for atoms removed both from cubic sites the energy gain is another 0.25 eV. The reason is an energy gain by larger relaxations due to Jahn-Teller distortions in the latter cases. Calculations done for the unrelaxed divacancies show that the total energy differs by less than 0.1 eV between different cases (see Table III). On the other hand, the energy lowering by Jahn-Teller distortion shows that the most favored case is ''cubcub'' followed by ''hexhex'' (see Table III).

Comparing the formation energies for divacancies, calculated here, to those for monovacancies we find the remarkable fact that divacancies formed from pure cubic or pure hexagonal lattice sites, i.e., situated along the c axis, are energetically more favorable by up to 0.6 eV than the corresponding Si monovacancies under equilibrium conditions for stoichiometric or C-rich material (see Table I).

Comparing to others, our results for 4H-SiC for the isolated carbon and silicon monovacancies in are very good agreement with the pseudopotential calculations by Zywietz *et al.*,[22] since in those calculations the same rectangular su-

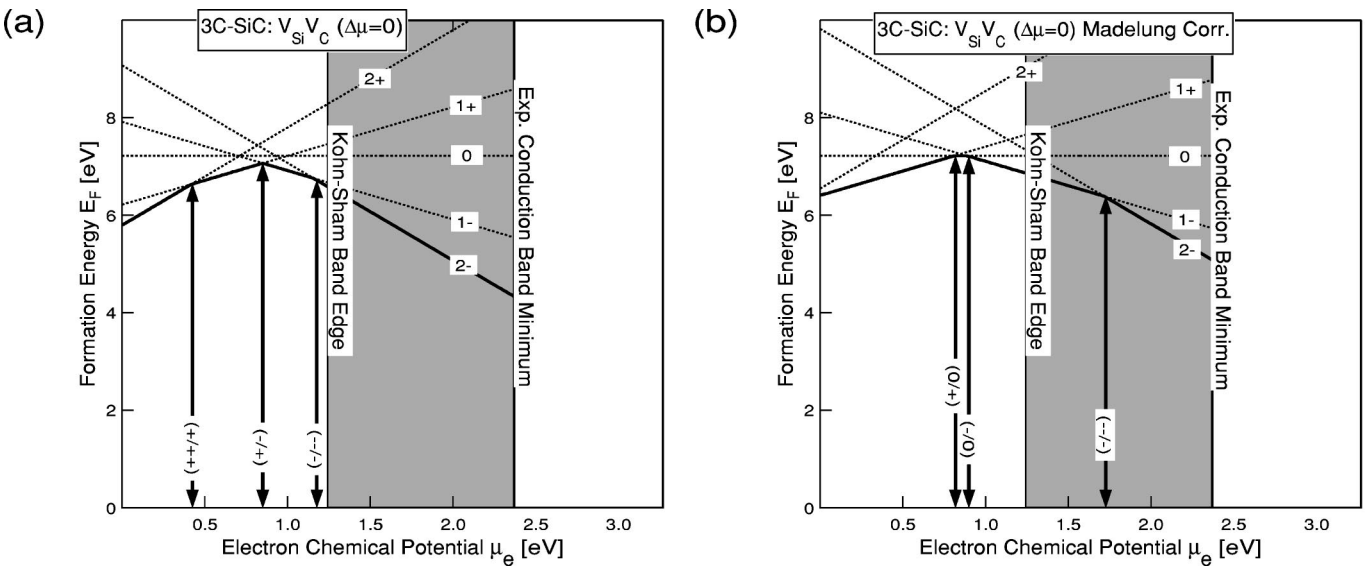

FIG. 3. $V_{Si}V_C$: divacancy in 3*C*-SiC for stoichiometric material ($\Delta\mu=0$). Formation energies E_F vs the electron chemical potential $\Delta\mu_e$ are given for different charge states (dashed lines), with each charge state indicated. The thick solid line corresponds to the lowest formation energy for all values of the Fermi level. The ionization levels are indicated in the picture. Note the negative-*U* effect found between charge states $(-/+)$ at the value of 0.85 eV of the electron chemical potential.

percell (128 atom) was used. However, Zywietz *et al.*[22] calculated the formation energy for the monovacancies in 3*C*-SiC in a 216-atom supercell. Thus in the case of the 3*C* structure their results should be more accurate due to a smaller defect-defect interaction.[39]

For 3*C*-SiC, we do not find such a good agreement for the formation energies of monovacancies with Wang *et al.*,[18] since they used only a 32-atom supercell, and no full ionic relaxations were allowed for. Hence, the values for the formation energies differ by up to 2 eV.

B. Ionization levels

The ionization levels for the divacancy in different configurations in 4*H*-SiC and in 3*C*-SiC are presented in Fig. 4(a) without the Madelung correction and in Fig. 4(b) with the Madelung correction applied. One observes that the negative-*U* behavior is removed in some cases (4*H*, cubcub, and hexhex, 3*C*) when the Madelung correction is applied.

Observations showing that the Z_1/Z_2 centers exhibit negative-*U* behavior in electron irradiated 4*H*- and 6*H*-SiC have been recently published.[6,40] Like the negative-*U* calculated for the divacancy, this negative-*U* transition is found between the charge states $1+$ and $1-$, but at a different position in the band gap. These centers have been identified in as irradiated and at 900 °C annealed samples. Therefore, it is quite probable that the observed signal is related to divacancies, since a divacancylike signal has been detected also by positron annihilation after similar sample preparation.[41,42]

In the tight-binding picture of $V_{Si}V_C$ by Talwar and Feng,[14] the one-electron levels were calculated to be at 0.48 eV and 1.62 eV above the VBM, and the symmetry character for the neutral divacancy was determined to be $E(C_{3v})$. It is found that for this divacancy symmetry, the two triply degenerate t_2-type isolated-impurity levels split and produce two sets of doubly degenerate *E*- or π-type bonds and two nondegenerate A_1 or σ-type levels.[14] Since the σ-type levels are derived from the mixing of *s*- and *p*-like orbitals of the two isolated defects, the A_1 states of the divacancy will be at energies significantly different from the two isolated vacancy states. In other words, the a_1-type resonance state of an isolated vacancy in the valence band can be pulled into the band gap by pairing it with an appropriate impurity. Hence, the earlier tight-binding calculations[14] suggest for the nearest-neighbor divacancy defects having C_{3v} symmetries, the possibility of localized impurity states to be detected in the gap. In this work, we find for the nearest-neighbor divacancy pair defects in the doubly positive- or negative-charge state a C_{3v} symmetry. For other charge states we calculate lower symmetries.

C. Relaxations

All studied divacancies in doubly positive- or negative-charge state exhibit a relaxation of the *breathing type* (sym-

TABLE III. Divacancies in 4*H*-SiC: We give the site dependence of the relaxation energies ΔE_{relax}, i.e., the total energy differences between unrelaxed and fully relaxed configurations, for all divacancy configurations in 4*H*-SiC.

	Formation energy		Relaxation energy
	Unrelaxed	Fully relaxed	
Defect	E_F [eV]	E_F [eV]	ΔE_{relax} [eV]
$V_{Si}^{cub}V_C^{cub}$	8.71	7.74	0.97
$V_{Si}^{cub}V_C^{hex}$	8.64	8.34	0.29
$V_{Si}^{hex}V_C^{hex}$	8.71	8.00	0.71

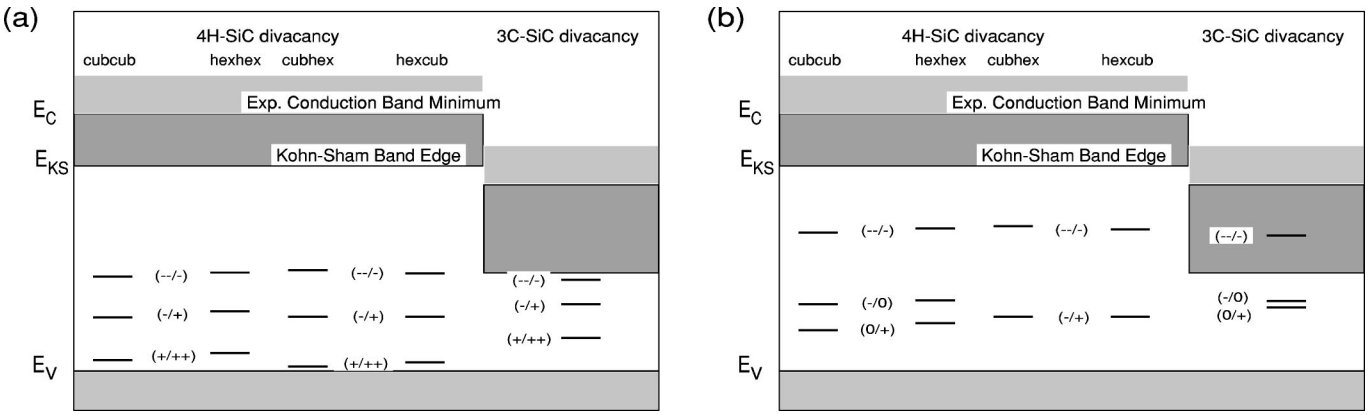

FIG. 4. Energy level schemes for Si-C divacancies in $4H$ as well as in $3C$-SiC, (a) without Madelung correction and (b) with Madelung correction. Results are given for all possible combinations of cubic and hexagonal lattice sites obtained from LSDA calculations employing a 128-atom supercell. In (b) highly positive-charged states are shifted by the Madelung correction into the valence band while highly negative-charge states move towards the conduction band.

metry point group C_{3v}). For single charge states we find a lower symmetry of *pairing-type* relaxations (C_{1h}). Provided that the neutral divacancy is found to be stable, we find a relaxation towards a *resonant-bond* structure (symmetry group C_{1h}).

The relaxations around the divacancy are comparable to the positively charged silicon or carbon monovacancies. There, as in the case of the divacancy, one dangling bond (one electron) is missing (see also Ref. 30 for the relaxation patterns). This means for the silicon atoms surrounding the missing C atoms that they cannot form two new bonds as in the case of the isolated C vacancy, since the fourth dangling bond is missing. Hence, nearly no inward relaxation is observed. The C atoms surrounding the missing silicon atom cannot form new bonds due to the too short bond length of diamond or graphite (see also the discussion in Ref. 30). Hence, they move outward—as for silicon monovacancies—and try to relax towards a more planar bonding configuration (π bonds) like in graphite. The relaxation patterns change slightly with the charge state as given in Table IV.

For divacancies in the pure cases, either cubic or hexagonal, a stronger inward or outward relaxation on the Si or C end of the divacancy is observed. This is obviously the reason for the clearly lower formation energies by 0.35 eV and 0.6 eV found for the pure hexagonal and pure cubic case, respectively. The lattice seems not to be able to change the bond length so much for neutral divacancies formed between mixed cubic and hexagonal lattice sites. Hence, it is more expensive to form a divacancy in the mixed configuration.

V. CONCLUSIONS

We have performed first-principles calculations for the electronic and ionic structure of the divacancy in $3C$- and $4H$-SiC. To correct for the electrostatic self-interaction arising from charged supercells, we employed the Madelung correction, in order to better compare experimentally obtained and calculated ionization levels. Even though the correction is known to be overestimated slightly, the correction does not affect the physics of the final results here.

While in the $3C$ polytype only one configuration exists, there are four different ones in $4H$-SiC due to atoms missing from a combination of cubic and hexagonal sites. In stoichiometric $4H$-SiC the formation energies for isolated vacancies in the charge-neutral state are about 4 eV on the carbon site V_C and about 8 eV on the silicon site V_{Si}. Hence, it is remarkable that such a low formation energy of about 8 eV for the divacancy $V_{Si}V_C$ in the charge-neutral state in $4H$-SiC is calculated.

We observe a clear site dependence, i.e., variations in the formation energy of up to 0.62 eV depending on the lattice sites (cubic or hexagonal) in which the defect complex is situated. This is related to the different possible energy-lowering relaxations. We find for all cases extraordinarily large binding energies of about 4 eV, which, in turn, imply that for almost all divacancy configurations $V_{Si}V_C$ their formation energy can even be up to 0.6 eV lower than the corresponding one for the isolated V_{Si} monovacancy. This means that the energy necessary for their dissociation is the binding energy plus the barrier for diffusion. Hence—once formed—they can be expected to be extremely stable defects.

The formation energy E_F for divacancies and silicon monovacancies in bulk SiC is much higher than that for the carbon monovacancy and for the antisites.[19,30] This indicates that the equilibrium divacancy concentration for stoichiometric semi-insulating material should be relatively low compared to antisites or carbon vacancies. Nevertheless, silicon monovacancies have been detected experimentally in as-grown material in different charge states. According to these facts one may speculate that in as-grown SiC divacancies may be the preferred defect species compared to isolated silicon monovacancies.

The divacancy in the $4H$ polytype can exist at different charge states $[+,-,--]$, where the neutral defect stabilizes only for some cases. Hence, we find a negative-U behavior between the charge states $1+$ and $1-$ for divacancies in $4H$-SiC situated on mixed sites (cubhex or hexcub), where

TABLE IV. Divacancies in 4*H*-SiC and 3*C*-SiC. Relaxations around the divacancy depend on its lattice sites, charge, and spin state. They are given in % of the ideal tetrahedral distances between NN carbon (distances d_{12}, d_{13}, d_{23}) or silicon atoms (distances d_{45}, d_{46}, d_{56}). In the last column we give the symmetry groups for some of the defects.

		Tetrahedral distances in [%] from ideal value						
		Carbon end			Silicon end			
Charge	Spin	d_{12}	d_{13}	d_{23}	d_{45}	d_{46}	d_{56}	Symm.
		4*H*-SiC: $V_{Si}^{hex}V_{C}^{cub}$						
2+	0	−0.1	0.0	+0.2	+10.3	+10.3	+9.7	C_{3v}
1+	1/2	−0.6	+0.4	+0.6	+9.1	+9.0	+8.2	C_{1h}
0	0	0.0	0.0	+0.2	+4.7	+4.6	+7.3	C_{1h}
1−	1/2	−2.3	+0.4	+0.6	+7.9	+7.9	+7.9	$\sim C_{1h}$
2−	0	−2.4	−0.1	+0.1	+8.0	+8.0	+8.6	S_2 ($\sim C_{3v}$)
		4*H*-SiC: $V_{Si}^{cub}V_{C}^{hex}$						
2+	0	+1.4	+1.4	+0.6	+8.8	+8.7	+8.9	C_{3v}
1+	1/2	+1.5	+1.6	−0.1	+7.0	+8.3	+8.5	C_{1h}
0	0	+0.6	+0.9	+0.9	+7.8	+4.6	+5.0	$\sim C_{1h}$
1−	1/2	+1.1	+1.2	−1.4	+6.2	+6.6	+6.8	C_{1h}
2−	0	−0.1	−0.2	−1.3	+6.0	+6.1	+6.3	$\sim C_{3v}$
		4*H*-SiC: $V_{Si}^{cub}V_{C}^{cub}$						
2+	0	+0.4	+0.3	+0.3	+8.3	+8.1	+8.0	$\sim C_{3v}$
1+	1/2	+0.1	+0.4	+0.6	+8.8	+7.9	+7.2	S_2
0	0	−0.3	−0.2	+1.1	+9.9	+6.3	+6.7	C_{1h}
1−	1/2	−0.8	+0.2	+0.5	+8.5	+8.0	+7.1	$\sim C_{1h}$
2−	0	−0.7	−0.5	−0.7	+8.5	+8.3	+7.8	$\sim C_{3v}$
		4*H*-SiC: $V_{Si}^{hex}V_{C}^{hex}$						
2+	0	−0.1	−0.0	+0.1	+9.0	+9.0	+8.6	$\sim C_{3v}$
1+	1/2	−0.3	+0.2	+0.2	+7.9	+7.9	+6.8	C_{1h}
0	0	−0.9	+0.9	−0.8	+4.7	+8.7	+5.6	C_{1h}
1−	1/2	−0.5	−0.2	−1.6	+5.9	+6.1	+5.5	C_{1h}
2−	0	−1.6	−1.6	−1.5	+5.6	+5.6	+5.4	$\sim C_{3v}$
	3*C*-SiC: $V_{Si}V_{C}$							
2+	0	+1.2	+1.2	+1.2	+11.3	+11.4	+11.4	$\sim C_{3v}$
1+	1/2	+0.9	+0.9	+1.5	+9.2	+9.2	+9.7	C_{1h} ($\sim C_{3v}$)
0	0	−0.3	+0.1	+2.2	+7.4	+7.5	+9.5	C_{1h}
1−	1/2	−0.7	+0.7	+0.8	+7.6	+8.0	+8.0	C_{1h}
2−	0	−0.4	−0.2	−0.2	+7.7	+7.9	+7.9	C_{3v}

the transitions occur at the same value of the electron chemical potential (0.7 eV above the VBM). Applying the Madelung correction for 3*C*-SiC the doubly negative-charge state moves above the Kohn-Sham band edge and, hence, it is doubtful if it can be observed. If the Madelung correction would slightly overestimate the shift in formation energies, there would be some room for the divacancy in 3*C*-SiC to exhibit a negative-*U* behavior as well, which would then be slightly higher in the band gap at about 0.85 eV above the VBM. For 4*H*-SiC, on the other hand, divacancies formed

along the *c* axis (cubcub or hexhex) have their neutral-charge state stabilized in a long range of the electron chemical potential and, hence, exhibit no negative-U behavior.

The relaxation pattern found around the divacancy can be described as follows: The nearest-neighbor silicon atoms at the carbon end of the $V_{Si}V_C$ hardly move at all from their ideal positions. On the other hand, the nearest-neighbor carbon atoms around the silicon end of the $V_{Si}V_C$ move symmetrically outward by about 10%, forming more sp^2-like bonds. The slightly different relaxations found for the divacancy in the pure cases (cubcub or hexhex) compared to those in the mixed cases (cubhex or hexcub) do indeed explain the differences in the formation energies observed.

ACKNOWLEDGMENTS

The authors wish to thank for the generous computing resources at the Center of Scientific Computing (CSC) in Espoo, Finland and at the National Supercomputer Center (NSC) in Linköping, Sweden. We wish to thank E. Janzén and all the other members of the Material Physics Group at the Linköping University (Sweden) for useful discussions. This work has been supported by Academy of Finland through its Centers of Excellence Program 2000-2005. T.E.M.S. acknowledges the support of a Marie-Curie Grant by the European Commission.

*Electronic address: Leena.Torpo@hut.fi
†Electronic address: tst@hugo.hut.fi
‡Electronic address: Risto.Nieminen@hut.fi

[1] H. Itoh, A. Kawasuso, T. Ohshima, M. Yoshikawa, I. Nashiyama, S. Tanigawa, S. Misawa, H. Okumura, and S. Yoshida, Phys. Status Solidi B **162**, 173 (1997).
[2] E. Sörman, N.T. Son, W.M. Chen, O. Kordina, C. Hallin, and E. Janzén, Phys. Rev. B **61**, 2613 (2000).
[3] T. Dalibor, G. Pensl, T. Kimoto, H. Matsunami, S. Sridhara, R.P. Devaty, and W.J. Choyke, Diamond Relat. Mater. **6**, 1333 (1996).
[4] G. Pensl and W.J. Choyke, Physica B **185**, 264 (1993).
[5] C. Hemmingsson, N.T. Son, O. Kordina, J.P. Bergman, E. Janzén, J.L. Lindström, S. Savage, and N. Nordell, J. Appl. Phys. **81**, 6155 (1997).
[6] C.G. Hemmingsson, N.T. Son, A. Ellison, J. Zhang, and E. Janzén, Phys. Rev. B **58**, R10 119 (1998).
[7] V.S. Vaĥner and V.A. Il'in, Sov. Phys. Solid State **23**, 12 (1981).
[8] W.J. Choyke, Z.C. Feng, and J.A. Powell, J. Appl. Phys. **64**, 3163 (1988).
[9] W.J. Choyke, Inst. Phys. Conf. Ser. **31**, 58 (1977).
[10] H. Itoh, M. Yoshikawa, I. Nashiyama, H. Okumura, S. Misawa, and S. Yoshida, J. Appl. Phys. **77**, 837 (1995).
[11] J.A. Freitas, S.G. Bishop, J.A. Edmond, J. Ryu, and R.F. Davis. J. Appl. Phys. **61**, 2011 (1987).
[12] T. Egilsson, A. Henry, I.G. Evanov, E. Janzén, and J.L. Lindström, Phys. Rev. B **59**, 8008 (1999).
[13] T. Egilsson, J.P. Bergman, I.G. Evanov, A. Henry, and E. Janzén, Phys. Rev. B **59**, 1956 (1999).
[14] D.N. Talwar and Z.C. Feng, Phys. Rev. B **44**, 3191 (1991).
[15] G. Brauer, W. Anwand, E.-M. Nicht, J. Kuriplach, M. Ŝob, N. Wagner, P.G. Coleman, M.J. Puska, and T. Korkonen, Phys. Rev. B **54**, 2512 (1996).
[16] G. Brauer, W. Anwand, P.G. Coleman, A.P. Knights, F. Plazaola, Y. Pacaud, W. Skorupa, J. Störmer, and P. Willutzki, Phys. Rev. B **54**, 3084 (1996).
[17] A. Polity, S. Huth, and M. Lausmann, Phys. Rev. B **59**, 10 603 (1999).
[18] C. Wang, J. Bernholc, and R.F. Davis, Phys. Rev. B **38**, 12 752 (1988).
[19] L. Torpo, S. Pöykkö, and R.M. Nieminen, Phys. Rev. B **57**, 6243 (1998).
[20] L.M. Torpo, R.M. Nieminen, K.E. Laasonen, and S. Pöykkö, Appl. Phys. Lett. **74**, 221 (1999).
[21] L. Torpo and R.M. Nieminen, J. Mater. Sci. Eng. B **61–62**, 593 (1999).
[22] A. Zywietz, J. Furthmüller, and F. Bechstedt, Phys. Rev. B **59**, 15 166 (1999).
[23] S. Pöykkö, M.J. Puska, and R.M. Nieminen, Phys. Rev. B **53**, 3813 (1996).
[24] M. Pesola, J. von Boehm, S. Pöykkö, and R.M. Nieminen, Phys. Rev. B **58**, 1106 (1998).
[25] D.M. Ceperley and B.J. Alder, Phys. Rev. Lett. **45**, 566 (1980).
[26] S.H. Vosko, L. Wilk, and M. Nusair, Can. J. Phys. **58**, 1200 (1980).
[27] R. Car and M. Parrinello, Phys. Rev. Lett. **55**, 2471 (1985).
[28] D. Vanderbilt, Phys. Rev. B **41**, 7892 (1990).
[29] G.B. Bachelet, D.R. Hamann, and M. Schlüter, Phys. Rev. B **26**, 4199 (1982).
[30] L. Torpo, M. Marlo, T.E.M. Staab, and R.M. Nieminen, J. Phys.: Condens. Matter **13**, 6203 (2001).
[31] W. H. Press, S. A. Teukolsky, W. T. Vetterling, and B. P. Flannery, *Numerical Recipes*, 1st ed. (Cambridge University Press, Cambridge, England, 1992).
[32] F. Tassone, F. Mauri, and R. Car, Phys. Rev. B **50**, 10 561 (1994).
[33] A. Williams and J. Soler, Bull. Am. Phys. Soc. **32**, 409 (1952).
[34] S. Pöykkö, M.J. Puska, and R.M. Nieminen, Phys. Rev. B **57**, 12 174 (1998).
[35] H. Monkhorst and J. Pack, Phys. Rev. B **13**, 5188 (1976).
[36] S.B. Zhang and J.E. Northrup, Phys. Rev. Lett. **67**, 2339 (1991).
[37] G. Makov and M.C. Payne, Phys. Rev. B **51**, 4014 (1995).
[38] J. Lento, M. Pesola, J.-L. Mozos, and R.M. Nieminen, Appl. Phys. Lett. **77**, 232 (2000).
[39] M.J. Puska, S. Pöykkö, M. Pesola, and R.M. Nieminen, Phys. Rev. B **58**, 1318 (1998).
[40] C.G. Hemmingsson, N.T. Son, and E. Janzén, Appl. Phys. Lett. **74**, 839 (1999).
[41] C.C. Ling, A.H. Deng, S. Fung, and C.D. Beling, Appl. Phys. A: Mater. Sci. Process. **70**, 33 (2000).
[42] C.C. Ling, C.D. Beling, and S. Fung, Phys. Rev. B **61**, 8016 (2000).